The contrasting behaviour of polycrystalline bulk gold and gold nanoparticle modified electrodes towards the underpotential deposition of thallium

Christopher Batchelor-McAuley, Gregory G. Wildgoose and Richard G. Compton

Received (in Durham, UK) 12th December 2007, Accepted 27th February 2008
First published as an Advance Article on the web 15th April 2008
DOI: 10.1039/b719208h

The underpotential deposition (UPD) of thallium onto a polycrystalline gold macroelectrode or gold nanoparticles (10 ± 5 nm in diameter) supported on multiwalled carbon nanotubes (MWCNTs) is compared both in the presence and the absence of adsorbed chloride anions. On the polycrystalline gold macrodisc electrode the UPD of thallium is observed. However, on the 10 nm gold nanoparticles supported on MWCNTs no UPD of thallium is observed despite several control experiments which confirmed that the gold nanoparticles were indeed electroactive. This is compared to the reported behaviour of larger 30–60 nm diameter gold nanoparticles at which UPD of thallium is also found to occur and the possible reasons for this are discussed. This report provides an example where the properties of metal nanoparticles differ markedly from the bulk metal and the properties of the nanoparticles vary significantly with the size of the nanoparticles.

1 Introduction

The underpotential deposition (UPD) of a monolayer of one metal (analyte) onto a different (substrate) metal at potentials more positive of the Nernst potential for bulk deposition has been studied on gold or gold/alloy electrodes for a wide variety of different systems including but not limited to: copper,[1,2] tellurium,[3] zinc,[4] palladium,[5] platinum,[6] nickel,[7] silver,[8] lead,[9–12] cadmium[9–11] and of most relevance to this report, thalium.[9–11,13] The majority of studies focus on UPD on the Au(111) crystal face, although UPD on other crystal faces and/or defect sites has also been shown to occur.[1,2,5–7] Both the adsorption and stripping processes can be affected by the presence of adsorbed anions, for example chloride, which can effect the observed peak potential of either or both steps.[1,4,13–15]

Under UPD conditions the adsorbed metal is usually deposited as a monolayer and this imparts more control over the deposition (in terms of allowing one to study the adsorption, nucleation and growth processes) than under bulk deposition conditions. Subsequently UPD is of interest in both physicochemical studies,[13,16] electroanalytical studies[12,17] (usually employing some form of stripping voltammetry) and also due to certain systems formed under UPD conditions exhibiting enhanced catalytic activity.[18–21]

The properties of metal nanoparticles are known to often differ from those of the bulk metal. For example, whilst gold is one of the most inert metals known gold nanoparticles are attracting considerable interest in industry as heterogeneous catalysts for a number of oxidation reactions carried out at relatively low (room) temperatures, and in academia where much remains unknown about the exact influence of the nanoparticles' size, morphology and the role of the support materials on the catalytic mechanisms—which are often unknown themselves.[22–24] Whilst it is recognized that the catalytic activity of gold nanoparticles is strongly dependant on their size (amongst other factors) little is still known about the exact shape and structure of gold nanoparticles of different sizes with varying claims of truncated octahedral, cub-octahedra, icosahedra, decahedra and amorphous structures made in the literature.[22] Catlow and co-workers have carried out computer simulations of the nucleation and growth of various nanoparticle structures and have determined the upper size limits before the nanoparticles are expected to exhibit properties of the bulk material.[25,26]

Recently we have investigated a variety of ways of supporting random arrays of gold nanoparticles ranging in size from 60 to 10 nm on carbon electrode substrates.[27–30] In the electroanalytical detection of ultra trace amounts of arsenic we have shown that multiwalled carbon nanotubes, heavily encrusted in 10 nm sized gold nanoparticles (AuCNTs), provide one of the most sensitive electrode materials for use in anodic stripping voltammetry.[30]

In this report we investigate the anodic stripping detection of thallium(I) at the same AuCNT modified electrodes (Au nanoparticle diameter 10 nm) and compare the response of the AuCNTs to that of a polycrystalline gold macrodisc electrode. No response is observed which would correspond to the UPD of Tl(I) on the AuCNT modified electrode, whilst the UPD of Tl(I) onto a polycrystalline gold macrodisc electrode are clearly evident. This is in contrast to larger gold nanoparticles (30–60 nm) supported on carbon nanotubes and glassy carbon spheres at which we have previously demonstrated the UPD of Tl(I) occurs and used it in the anodic stripping voltammetric detection of thallium.[27]

Physical and Theoretical Chemistry Laboratory, Oxford University, South Parks Road, Oxford, UK OX1 3QZ. E-mail: richard.compton@chem.ox.ac.uk; Fax: +44 (0)1865 275410; Tel: +44 (0)1865 275413

2 Experimental

2.1 Reagents and equipment

All reagents were purchased from Aldrich (Gillingham, UK) with the exception of potassium chloride (Reidel de Häen, Seelze, Germany). "Bamboo-like" multiwalled carbon nanotubes (b-MWCNTs) were purchased from Nanolab (Brighton, MA, USA)[31] and consist of tubes 30 ± 15 nm in diameter and 2–20 μm in length. The term "bamboo-like" refers to the fact that the tubes are periodically closed along their length similar to the structure of bamboo from which the name derives.

Electrochemical measurements were recorded using a computer controlled μAutolab potentiostat (EcoChemie) with a standard three-electrode configuration in solutions containing 0.1 M KCl as supporting electrolyte. Either a polycrystalline gold macrodisc (diameter 1.0 mm) or basal plane pyrolytic graphite electrode (bppg, 5 mm diameter, Le Carbone, Sussex, UK) acted as the working electrode (see below). A platinum wire (99.99% GoodFellow, Cambridge, UK) counter electrode and a saturated calomel reference electrode (SCE, Radiometer, Copenhagen, Denmark) completing the cell assembly. The gold electrode surface was renewed where necessary by polishing using an alumina slurry of decreasing particle size (1.0–0.3 μm) and sonicated in ethanol between polishing to remove any adhered alumina. The bppg electrode surface was renewed where necessary by pressing the electrode surface onto sellotape and gently peeling away the top few layers of graphite. Finally the bppg electrode was rinsed in acetone to remove any adhesive from the sellotape. All experiments were carried out at 20 ± 2 °C.

Transmission electron microscopy (TEM) was performed on a JEOL 2000FX microscope with a tungsten filament as electron source; an acceleration voltage of 200 kV was applied.

2.2 Preparation of gold modified multiwalled carbon nanotubes

The procedure used for modification of the b-MWCNTs was adapted from reports previously published.[32] First 50 mg of the b-MWCNTs were activated by refluxing in a 3 M solution of HNO_3–H_2SO_4 (1 : 1) at 80 °C for 5 h and washed thoroughly with pure water. Next the b-MWCNTs were suspended in a 1 mg mL^{-1} aqueous suspension containing 1% sodium dodecyl sulfate (SDS) surfactant and sonicated for 30 min. Finally gold nanoparticles were deposited onto the activated b-MWCNTs by mixing the suspension with 500 μL of 1% $HAuCl_4 \cdot H_2O$ followed by 500 μL of 0.75% $NaBH_4$ added dropwise while stirring. The mixture was stirred for another 5 min then filtered with Millipore membrane filter (0.45 μm, Millipore) and washed with pure water. Characterisation of the gold nanoparticle modified b-MWCNTs (AuCNTs) was performed using transmission electron microscopy and confirmed that the b-MWCNTs are heavily encrusted in gold nanoparticles with an average diameter of 10 ± 5 nm (Fig. 1).

2.3 Modification of a bppg electrode

In order to immobilise the AuCNTs onto the surface of a clean bppg electrode a "casting" solution of 1 mg mL^{-1} of the AuCNTs suspended in chloroform and sonicated for 30 min was used. A 20 μL aliquot of this casting suspension was then placed onto the bppg electrode surface and the solvent allowed to evaporate at room temperature leaving the AuCNTs immobilized onto the bppg surface.

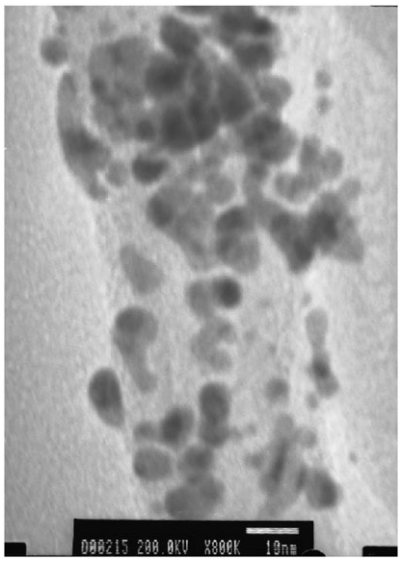

Fig. 1 A TEM image showing the gold nanoparticles encrusting a b-MWCNT.

3 Results and discussion

3.1 Voltammetric characterisation

The presence of gold on the AuCNT modified bppg electrode was characterised by performing cyclic voltammetry in 0.1 m H_2SO_4 from 0.0 to +1.6 V (*vs.* SCE) at a scan rate of 100 mV s^{-1}. The formation of gold oxides on the oxidative scan is obscured by the onset of solvent breakdown. However, on the reverse scan a clear reduction peak is observed at around +0.85 V corresponding to the reduction of the gold surface oxides formed in the forward scan. The area of this peak is proportional to the total electroactive surface area of gold nanoparticles on the electrode in a ratio of 390 μC cm^{-2} which is the value derived from bulk gold surfaces.[33] The electroactive area of gold on the surface of the AuCNT modified bppg electrode was reproducibly found to be 0.06 ± 0.01 cm^2 which is almost ten times larger than that of the gold macrodisc electrode despite the amount of AuCNTs immobilised onto the bppg surface being so small.

3.2 Comparing the UPD of Tl(I) on polycrystalline macrodisc and gold nanoparticle electrodes

The UPD of Tl(I) on the gold macrodisc was examined using cyclic voltammetry in 0.1 M HNO_3 as shown in Fig. 2. Both the gold oxide reduction peak at +0.67 V *vs.* SCE and the UPD of Tl(I) at −0.29 V are visible in the reductive scan. If the potential is then swept in the oxidising direction the corresponding thallium stripping peak is observed at −0.21 V. However, when this experiment was repeated with the AuCNTs only the gold oxide reduction peak was seen with

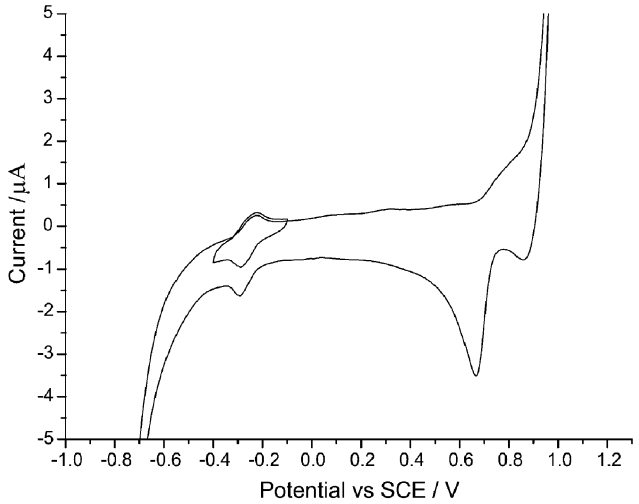

Fig. 2 The overlaid cyclic voltammograms recorded over the range −0.7 to 1.0 V and the second scan over the thallium UPD and stripping region of a gold macroelectrode in 0.1 M HNO_3 and 0.25 mM $TlNO_3$ at a scan rate of 100 mV s^{-1}.

no well defined voltammetric signals corresponding to either the UPD or stripping of thallium observed.

If the deposition potential is held at −1.2 V *vs.* SCE which is sufficiently negative to drive the bulk deposition of thallium then a bulk thallium stripping peak is observed at –0.64 V at both the polycrystalline gold macrodisc electrode and the AuCNT modified bppg electrode (Fig. 3). However, a control experiment using unmodified MWCNTs immobilised onto a bppg electrode reveals a stripping peak at −0.65 V, indicating that the bulk deposition of thallium occurs on the underlying carbon substrates as well as on the gold nanoparticles (the stripping peak itself is rather broad and may be a composite peak of thallium stripping from the bppg, MWCNTs and the gold nanoparticles). Thus the AuCNTs offer no analytical advantage for the bulk detection of thallium.

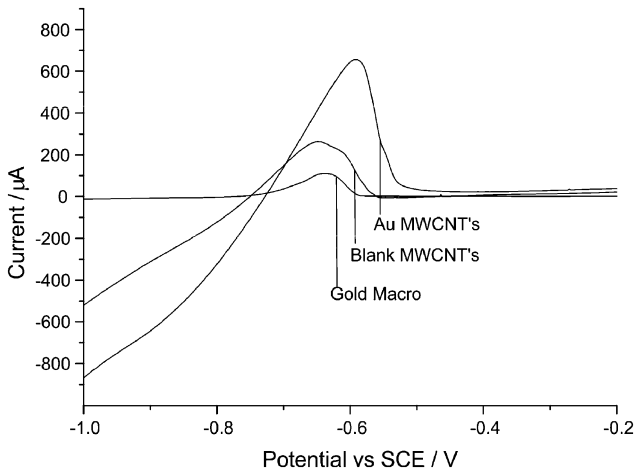

Fig. 3 The LSASV of a bare gold macroelectrode run, a bppg electrode modified with bare MWCNTs and a bppg electrode modified with AuCNTs in 0.1 M HNO_3 and 0.25 mM $TlNO_3$ with thallium deposited for 300 s at the bulk deposition potential of −1.2 V. Scan rate of 100 mV s^{-1}.

Linear sweep anodic stripping voltammetry (LSASV) was performed using the UPD of Tl(I) on a gold macrodisc electrode by poising the electrode potential at −0.5 V *vs.* SCE for 30 s and then scanning from −0.5 to +0.3 V at 100 mV s^{-1} in 0.1 M HNO_3 (Fig. 4(a)). Standard additions of thallium(I) nitrate were performed over the range 0–8 μM with 1.0 μM additions and over the range 0–2.0 μM with 0.2 μM additions, the corresponding standard addition plots of peak area (charge) *vs.* concentration of Tl(I) are shown in Fig. 4(b) and (c). At low concentrations of Tl(I) the limit of detection (determined using 3σ) was found to be 0.22 μM which

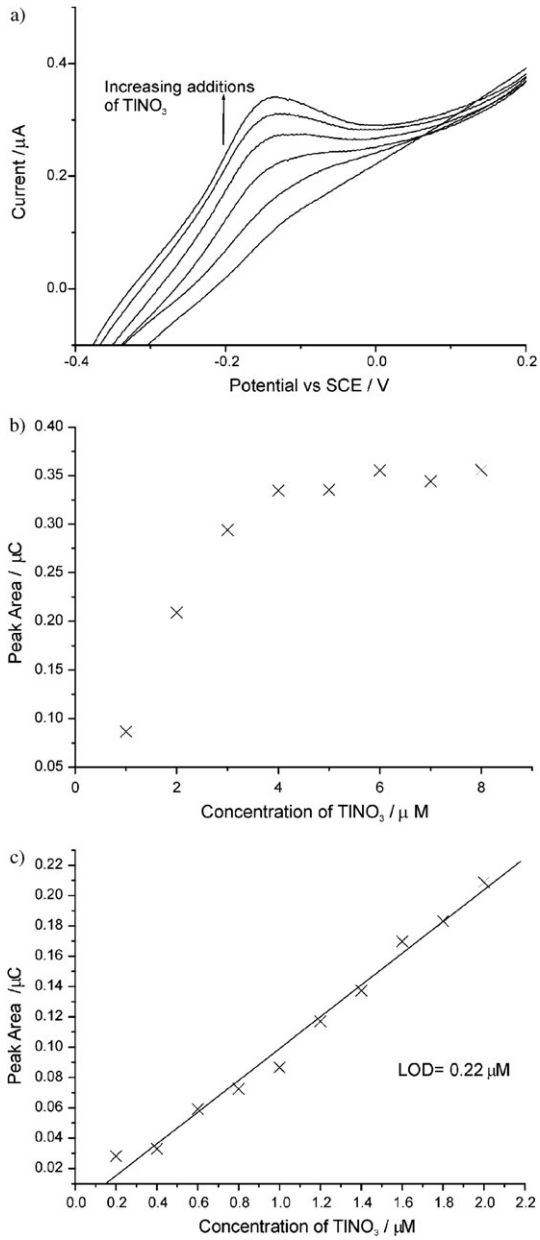

Fig. 4 (a) The LSASV of a gold macroelectrode in 0.1 M HNO_3 with increasing concentrations of $TlNO_3$ (1 μM increments). The standard addition plots of peak area *vs.* concentration at (b) high thallium concentration and (c) lower thallium concentrations. Data recorded using the UPD of thallium at a deposition potential of −0.5 V *vs.* SCE for 30 s. Scan rate 100 mV s^{-1}

compares favourably to the literature.[27] Above *ca.* 4 μM the peak area limits indicating that the all the available sites for UPD are occupied. The charge passed is easily related to the number of thallium atoms deposited *via* the Faraday law. Using the van der Waals radius of thallium atoms (196 pm) and ignoring any possible contribution from co-adsorbed anions, the area of the gold electrode covered by the deposited thallium monolayer is 33% of the total surface area of the electrode. The polycrystalline gold surface predominantly consists of three crystal faces, Au(100), Au(110) and Au(111) which should, on average, each comprise approximately one third of the total surface. There are two possible explanations for this behaviour. The first is that the thallium adatoms are preferentially being deposited on only one crystal face. In light of the fact that the UPD of thallium has been shown to occur on the Au(111) surface, we speculate that this crystal face onto which thallium UPD occurs may be the preferred site of UPD, although we note that this argument is based mainly on the prevalence of Au(111) studies in the literature and the parsity of studies on other crystal faces which may be equally or even more favourable for Tl UPD. The second more likely explanation is that, due to the mismatch in the size of the thallium and gold atoms the thallium UPD layer can not form a close-packed monolayer of thallium adatoms on the gold terraces. The layer of thallium formed during UPD is only deposited on those terraces that are large enough to accommodate an incommensurate adlayer leading to incomplete surface coverage.

The above experiments were also repeated using the AuCNTs but even at the highest Tl(I) concentrations used no stripping peak was observed. Again this could be interpreted as being due to a total lack of Au(111) faces of sufficient size to support the adlayer of thallium. More probably, clearly defined terraces of any crystal face may not be present due to the small size of the gold nanoparticles. In other words there may not be sufficient areas of terraces to support the incommensurate adlayer and any thallium atoms deposited are located on a range of different sites including steps, kinks and terrace defects. As the UPD is highly sensitive to surface structure the stripping of small numbers of surface bound adatoms from this more disordered surface structure may occur over a wider range of potentials. This would consequently produce a smaller, broader stripping peak which may not be discernable from the background capacitance.

3.3 Comparing the UPD of Tl(I) on polycrystalline macrodisc and gold nanoparticle electrodes in the presence of added chloride anions

We note that in our previous studies using slightly larger gold nanoparticles (30–60 nm in diameter) in the presence of added chloride ions we did obtain useful analytical signals for Tl(I) corresponding to UPD onto gold nanoparticles.[27] It has been reported in the literature that the presence of adsorbed anions such as chloride on the surface of gold electrodes can influence the UPD and stripping potentials of thallium.[13] Therefore the UPD LSASV experiments described above were repeated using 10 mM HNO_3 + 10 mM NaCl as supporting electrolyte.[13,27] Fig. 5 shows the resulting LSASV with a deposition potential of −0.5 V was applied for 30 s as before. The stripping peak potential has shifted in the presence of chloride to −0.24 V *vs.* SCE, again in agreement with the literature,[13] and the limit of detection obtained at the gold macrodisc electrode in this electrolyte was improved to 0.143 μM (based on 3σ, inset Fig. 5).

Montes-Rojas and Chainet,[13] in their investigation into the effect of Cl^- anions on the UPD of Tl(I) on gold, noted that the stripping peak of Tl(I) corresponding to UPD consisted of several waves. Therefore, the deposition potential was decreased slightly to −0.8 V (still more positive than the onset of overpotential bulk deposition of thallium) for 30 s and the LSASV was performed between −0.8 and +0.5 V *vs.* SCE, again in 10 mM HNO_3 and 10 mM NaCl. Now a second stripping wave is observed at −0.45 V in excellent agreement with Montes-Rojas and Chainet (Fig. 6).[13] Again the thallium stripping peak was found to limit above a thallium concentration of *ca.* 6 μM. This is a slightly higher limiting concentration than that seen in the absence of any chloride (4 μM), however the peak area (and hence surface coverage of thallium adatoms) is similar in both cases indicating that the proportion of the macrodisc electrode comprising the active crystal face is almost constant despite the electrode being polished between experiments.

The above experiments were once more repeated using the AuCNTs supported on a bppg electrode, in order to see if the presence of chloride had any effect on the UPD of Tl(I) onto the gold nanoparticles. Once again no voltammetry corresponding to the stripping or UPD of thallium could be observed even at the highest concentration of Tl(I) studied.

As a further control experiment to demonstrate that the gold nanoparticles were indeed present on the electrode surface and still electroactive for the deposition and stripping of metals, we examined the response of the AuCNTs and the gold macroelectrode to a 3 mM solution of As(III) in 0.2 M HCl containing an addition 0.1 M KCl. A deposition potential of −0.4 V *vs.* SCE was applied for 240 s before performing LSASV from −0.4 to +0.5 V at a scan rate of 100 mV s^{-1}.

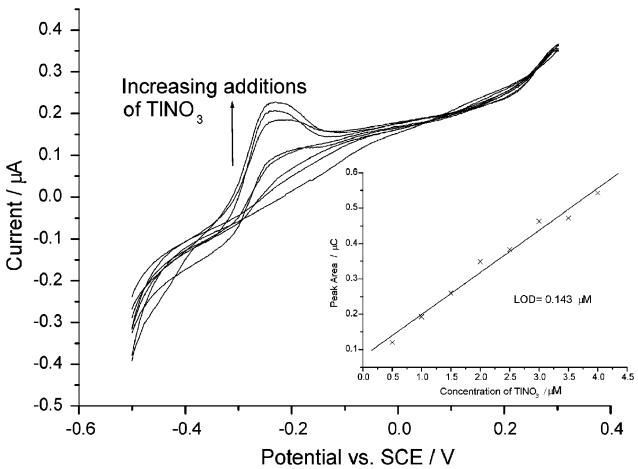

Fig. 5 The LSV of a gold macroelectrode in 10 mM NaCl and 10 mM HNO_3 with 0.5 μM additions of $TlNO_3$. Thallium deposited at −0.5 V for 30 s. Inset shows plot of peak area *versus* concentration. Scan rate 100 mV s^{-1}.

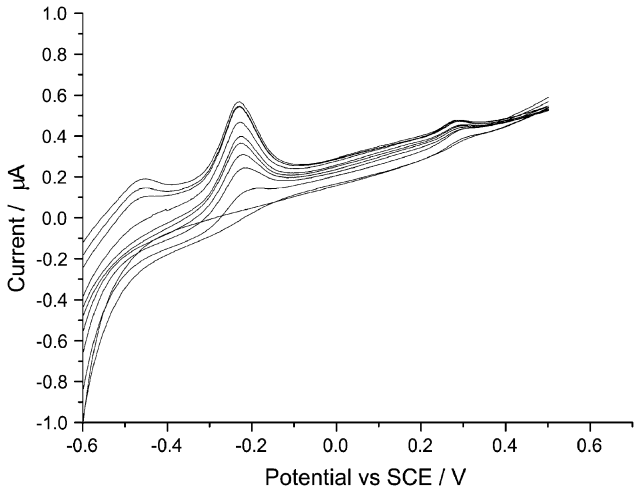

Fig. 6 The LSV of a gold macroelectrode in 10 mM NaCl and 10 mM HNO_3 with 1 μM additions of $TlNO_3$. Deposition potential −0.8 V for 30 s. Scan rate 100 mV s^{-1}.

In both cases a stripping peak could be observed at *ca.* 0.20 V corresponding to the stripping of arsenic from the gold nanoparticles or gold macrodisc electrode (Fig. 7). Note that arsenic has been shown not to deposit on the carbon support materials under these conditions and only deposits on the electroactive gold regions of the electrode. The stripping peak in the case of the AuCNTs is much larger and sharper than the gold macrodisc electrode in agreement with our recent studies of As(III) detection at AuCNT electrodes which has shown that they are ultra-sensitive to As(III), and possess a larger electroactive surface area than bulk gold electrodes.[30]

Finally, in order to identify the presence of any Au(111), Au(110) or Au(100) terraces on the gold nanoparticles we attempted the UPD of lead(II) following the method of Hernández *et al.*[12] Interestingly, once again no voltammetric features corresponding to the UPD of lead could be observed for the 10 nm gold nanoparticles, and only a OPD peak could be observed which our control experiments showed to be the deposition of lead on the MWCNTs and underlying bppg substrate in addition to on the gold nanoparticles. Thus, it is still not clear whether these 10 nm gold nanoparticles simply do not possess enough of the active crystal face(s) at which the UPD of metals such as thallium or lead occur, or whether, the structure of the smaller nanoparticles is sufficiently disordered that terraces of a size capable of accommodating sufficient adlayers of deposited metal adatoms to be voltammetrically observable.

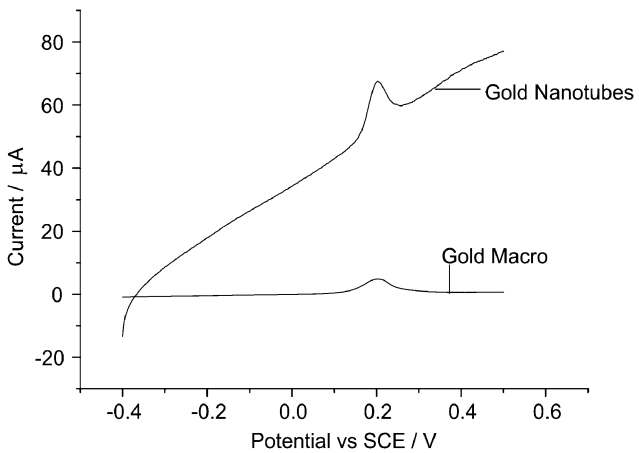

Fig. 7 The LSV of gold macro and gold MWCNTs in 0.2 M HCl, 0.1 M KCL and 3 mM As(III). Scan rate 100 mV s^{-1}.

What is clear is that the AuCNTs are electroactive and in fact possess a greater electroactive surface area than the polycrystalline gold macrodisc electrodes. The larger 30–60 nm gold nanoparticles, studied previously,[28] clearly do have active crystal surfaces upon which thallium UPD can occur. This provides an interesting example whereby the properties of the gold material are strongly size dependent.

4 Conclusions

The UPD of thallium on both a polycrystalline gold macrodisc electrode and on gold nanoparticles supported on MWCNTs has been studied in the presence and absence of chloride anions. It has been shown that in both cases the UPD of thallium occurs on polycrystalline gold macroelectrodes but the adlayer of thallium atoms only covers approximately 33% of the total surface area of the polycrystalline gold macrodisc electrode. A rigorous comparison with gold single-crystal electrodes is currently unavailable to us; as such this paper is intended to stimulate further research into this area. The UPD of thallium does not occur on gold nanoparticles which are 10 ± 5 nm in diameter either in the presence or absence of chloride ions. This suggests that gold nanoparticles of this size do not possess significant active crystal faces of sufficient size upon which the UPD of thallium can occur. This is in contrast to larger 30–60 nm diameter gold nanoparticles on which we have previously shown the UPD of thallium does occur. Thus the properties of nanometre sized gold particles can be strongly influenced by the size and structure of the nanoparticles and can differ markedly from the properties of bulk gold.

Acknowledgements

G. G. W. thanks St John's College, Oxford, for a Junior Research Fellowship. The authors are grateful to Mr Lei Xiao, PTCL, Oxford University for his assistance in obtaining the TEM image.

References

1 M. Seo and M. Yamazaki, *J. Solid State Electrochem.*, 2007, **11**, 1365–1373.
2 M. Nielinger, P. Berenz, X. Xiao and H. Baltruschat, *Surf. Sci.*, 2005, **597**, 1–10.
3 W. Zhu, J. Y. Yang, D. X. Zhou, S. Q. Bao, X. A. Fan and X. K. Duan, *Electrochim. Acta*, 2007, **52**, 3660–3666.
4 R. Marczona and K. Varga, *J. Radioanal. Nucl. Chem.*, 2006, **269**, 29–42.
5 F. Hernandez and H. Baltruschat, *Langmuir*, 2006, **22**, 4877–4884.
6 A. Kongkanand and S. Kuwabata, *J. Phys. Chem. B*, 2005, **109**, 23190–23195.
7 A. Vaskevich, F. Sinapi, Z. Mekhalif, J. Delhalle and I. Rubinstein, *J. Electrochem. Soc.*, 2005, **152**, C744–C750.
8 Y.-C. Liu, *Langmuir*, 2003, **19**, 6888–6893.

9 B. Krasnodębska-Ostrega, J. Pałdyna and J. Golimowski, *Electroanalysis*, 2007, **19**, 620.
10 B. Krasnodębska-Ostrega and J. Piekarska, *Electroanalysis*, 2005, **17**, 815.
11 Y. Bonfil, M. Brand and E. Kirowa-Eisner, *Electroanalysis*, 2003, **15**, 1369–1376.
12 F. Hernández, J. Solla-Gullón and E. Herrero, *J. Electroanal. Chem.*, 2004, **574**, 185.
13 A. Montes-Rojas and E. Chainet, *J. Mexican Chem. Soc.*, 2005, **49**, 336–343.
14 G. Horanyi and G. Vertes, *J. Electroanal. Chem.*, 1973, **74**, 705.
15 N. Markovic and P. N. Ross, *Langmuir*, 1993, **9**, 580.
16 E. Kirowa-Eisner, Y. Bonfil, D. Tzur and E. Gileadi, *J. Electroanal. Chem.*, 2003, **552**, 171–183.
17 G. Herzog and D. W. M. Arrigan, *TrAC, Trends Anal. Chem.*, 2005, **24**, 208–217.
18 R. Adzic, *Electrocatalysis*, Wiley-VCH, New York, 1998.
19 T. S. Ahmadi, Z. L. Wang, A. Henglein and M. A. El-Sayed, *Chem. Mater.*, 1996, **8**, 1161–1163.
20 J. W. Yoo, D. J. Hathcock and M. A. El-Sayed, *J. Catal.*, 2003, **214**, 1–7.
21 M. S. El- Deab and T. Ohsaka, *Electrochem. Commun.*, 2002, **4**, 288–292.
22 M. B. Cortie and E. van der Lingen, *Mater. Sci. Forum*, 2002, **26**, 1–14.
23 R. Grisel, K.-J. Weststrate, A. Gluhoi and B. E. Nieuwenhuys, *Gold Bull.*, 2002, **35**, 39–45.
24 T. K. Sau, A. Pal and T. Pal, *J. Phys. Chem. B*, 2001, **105**, 9266–9272.
25 M. J. Mora-Fonz, S. Hamad and C. R. A. Catlow, *Mol. Phys.*, 2007, **105**, 177–187.
26 S. Hamad, C. R. A. Catlow, S. M. Woodley, S. Lago and J. A. Mejias, *J. Phys. Chem. B*, 2005, **109**, 15741–15748.
27 X. Dai, G. G. Wildgoose and R. G. Compton, *Analyst*, 2006, **131**, 1241–1247.
28 X. Dai, G. G. Wildgoose, C. Salter, A. Crossley and R. G. Compton, *Anal. Chem.*, 2006, **78**, 6102–6108.
29 I. Streeter, L. Xiao, G. G. Wildgoose and R. G. Compton, *J. Phys. Chem. C*, 2008, **112**, 1933–1937.
30 L. Xiao, G. G. Wildgoose and R. G. Compton, 2007, submitted.
31 http://www.nanolab.com.
32 M. Zhang, L. Su and L. Mao, *Carbon*, 2006, **44**, 276.
33 S. Trasatti and O. Petrii, *Pure Appl. Chem.*, 1991, **63**, 711.

